ANNUAL REVIEWS

Annual Review of Biophysics

Imaging mRNA In Vivo, from Birth to Death

Evelina Tutucci,[1] Nathan M. Livingston,[2,3] Robert H. Singer,[1,4,5] and Bin Wu[2,3,6]

[1]Department of Anatomy and Structural Biology, Albert Einstein College of Medicine, Bronx, New York 10461; email: evelina.tutucci@einstein.yu.edu, robert.singer@einstein.yu.edu

[2]Center for Cell Dynamics, Johns Hopkins School of Medicine, Baltimore, Maryland 21205

[3]Department of Biophysics and Biophysical Chemistry, Johns Hopkins School of Medicine, Baltimore, Maryland 21205

[4]Gruss-Lipper Biophotonics Center, Albert Einstein College of Medicine, Bronx, New York 10461

[5]Cellular Imaging Consortium, Janelia Research Campus, Howard Hughes Medical Institute, Ashburn, Virginia 20147

[6]The Solomon H. Snyder Department of Neuroscience, Johns Hopkins School of Medicine, Baltimore, Maryland 21205; email: nliving5@jhmi.edu, bwu20@jhmi.edu

Annu. Rev. Biophys. 2018. 47:85–106

First published as a Review in Advance on January 18, 2018

The *Annual Review of Biophysics* is online at biophys.annualreviews.org

https://doi.org/10.1146/annurev-biophys-070317-033037

Keywords

single-mRNA imaging, gene expression, single-molecule, kinetics, imaging, single-cell

Abstract

RNA is the fundamental information transfer system in the cell. The ability to follow single messenger RNAs (mRNAs) from transcription to degradation with fluorescent probes gives quantitative information about how the information is transferred from DNA to proteins. This review focuses on the latest technological developments in the field of single-mRNA detection and their usage to study gene expression in both fixed and live cells. By describing the application of these imaging tools, we follow the journey of mRNA from transcription to decay in single cells, with single-molecule resolution. We review current theoretical models for describing transcription and translation that were generated by single-molecule and single-cell studies. These methods provide a basis to study how single-molecule interactions generate phenotypes, fundamentally changing our understating of gene expression regulation.

Contents

INTRODUCTION

Methods to follow single-cell dynamics over long periods of time are critical to revealing rare, heterogeneous, and dynamic cellular responses that can be confounded by ensemble measurements. Single-cell and multicellular organisms often rely on subtle changes in gene expression patterns to decide the fate of a single cell as a unit or as part of a multicellular network. However, because gene expression is a multistep process consisting of sequential stochastic single-molecule events, sporadic variations can be difficult to distinguish by the intrinsic variations in gene expression or so-called noise (93, 109). In recent years, we have seen the development of imaging techniques to visualize messenger RNAs (mRNAs) and proteins with single-molecule resolution allowing the study of gene expression regulation with unprecedented temporal and spatial precision. This is due to major progress made in the fluorescence microscopy field and to the development of molecular probes used to label proteins and nucleic acids (96, 108).

The combination of biochemical studies with imaging techniques in fixed cells allows for the identification of factors controlling gene expression and how variable this process is from cell to cell. However, lack of temporal resolution limits the study of the relationship of the components of transcription, processing, nuclear export, localization, translation, and degradation. The introduction of single-molecule imaging in living cells brings new insights and perspectives as to how these different steps of gene expression are dynamically interconnected. Development of theoretical models describing the kinetics of mRNA and protein production have clarified how macroscopic output emerges from single-molecule interactions (69, 143).

VISUALIZATION OF SINGLE mRNAs

Multiple optical techniques have been implemented to visualize mRNA in situ. Studying the subcellular localization of mRNA in both fixed (40) and live cells (8) has provided insights on the kinetics of transcription (31, 150), mRNA export (50), and translation (143). From fixed to live

cells, this section explores the most recent methods in imaging the life of mRNA from cradle to grave.

Fixed-Cell Imaging: smFISH and Beyond

Single-molecule fluorescence in situ hybridization (smFISH) has long been the standard in localizing individual mRNAs in fixed samples (40). Detection of single transcripts relies on a robust, multivalent signal from an array of fluorophore-tagged oligodeoxynucleotides (ODNs) hybridizing to an mRNA of interest in single eukaryotic and prokaryotic cells (**Figure 1*a***) (39, 40, 105). Significant improvements to probe design and hybridization conditions have increased speed, sensitivity, and specificity to a point where individual allelic variants, single-nucleotide polymorphisms, or RNA editing can be identified (57, 84, 115). Branched DNAs also offer significant signal amplification by conjugating an array of secondary DNA probes to a primary ODN with a region of homology to the target gene (**Figure 1*b***) (5). Improved tissue preparation techniques demonstrated that multiple genes can be monitored in whole-mount *Drosophila melanogaster* brains (78, 147), in intact mammalian liver, or in intestinal epithelium (53, 87).

Simultaneous detection of multiple RNAs in the same cell through combinatorial barcoding (multiplexed smFISH) revealed global population heterogeneity in mRNA expression and that many mRNA species have specific localization patterns (72, 80). Combinatorial labeling plus sequential rounds of hybridization expanded the potential of multiplexed smFISH (**Figure 1*c***) (22, 81, 86), and simultaneous imaging of over 1,000 RNA species in single cells has been achieved (22). In particular, multiplexed error-robust FISH (MERFISH) mitigated the relatively high error rate associated with sequential hybridization by employing a novel error-correcting coding scheme and demonstrated the potential to cover the complete transcriptome profile of a cell (22, 86).

Interpretation of mRNA copy number and localization in smFISH experiments requires significant computational analysis. Programs such as FISH-quant (91) and Airlocalize (75) avoid experimental bias by automatically scoring mRNA abundance in the nucleus or cytoplasm. However, copy number and localization are not the only parameters for assessing mRNA functionality. Protein and mRNA interactions provide crucial insights into regulatory mechanisms. smFISH coupled with immunofluorescence can identify the messenger ribonucleoparticles (mRNPs) characteristic of each stage in the lifetime of an mRNA (37, 144). Significant improvement in the colocalization precision was achieved through the development of a superregistration method. This approach calibrates and corrects for chromatic aberrations to distinguish bona fide RNA–protein interactions in situ (37). Despite the wealth of information available using these fixed-cell methods, live-cell techniques offer further information about the regulation of gene expression by adding the crucial time dimension.

Live-Cell Techniques: mRNA Movement and Expression in Space and Time

Live-cell imaging techniques allow the study of mRNA expression dynamics in real time. Individual mRNA molecules can be visualized in living cells through probe hybridization to the endogenous transcript or through engineering of the target mRNA.

Molecular beacons (MBs) are probes used to target endogenous transcripts (139). These single-stranded DNA molecules fold into a native stem-loop structure connected to a complementary sequence to an RNA of interest (**Figure 1*d***). One end of the stem-loops contains a fluorescent molecule while the other contains a quencher (139). Upon hybridization with high target sequence specificity, the fluorescent moiety and quencher are separated and light is emitted. However, because these probes do not penetrate cells, they require microinjection or introduction by some

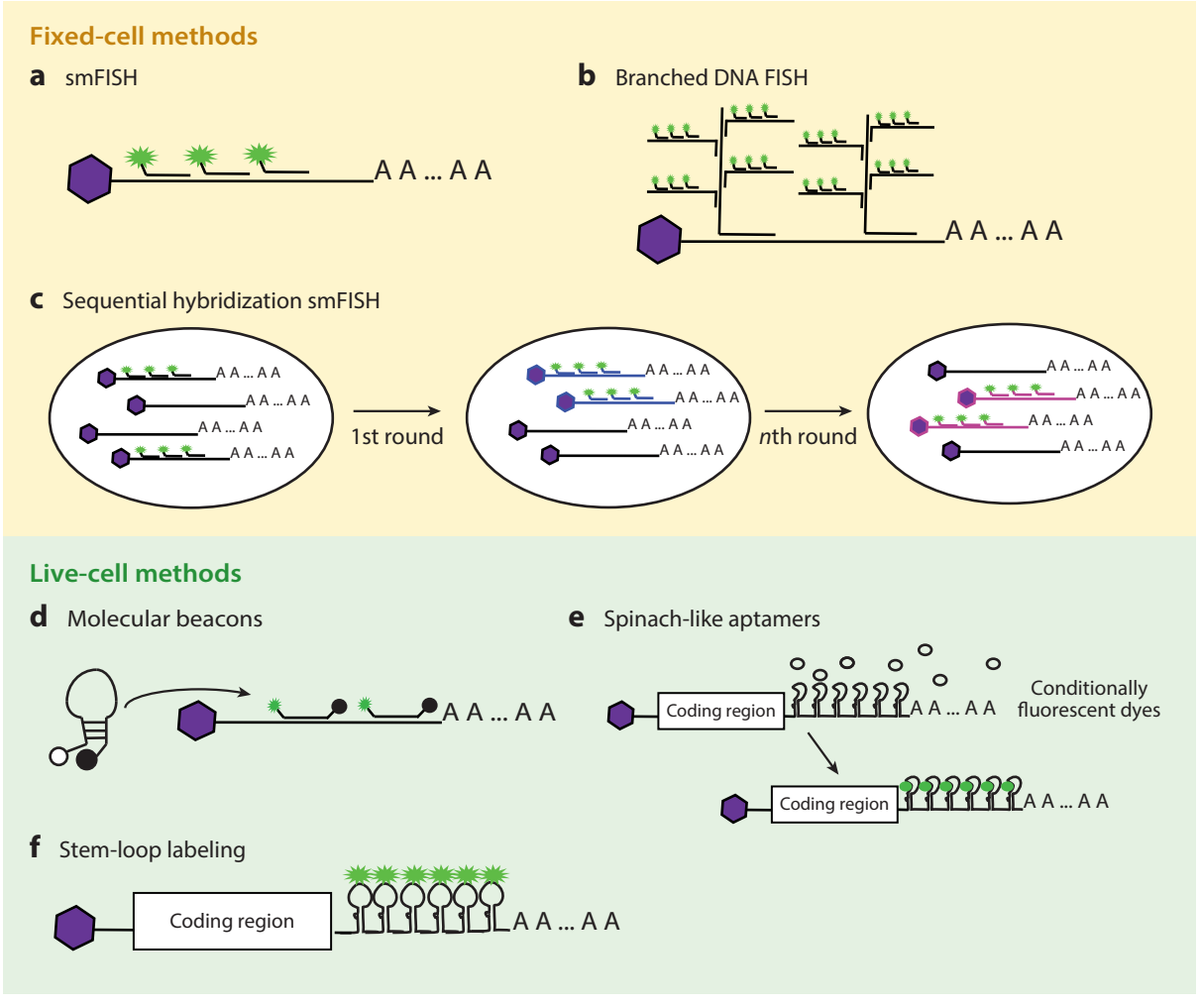

Figure 1

Methods in messenger RNA (mRNA) imaging. Fixed cells (panels *a–c*) versus living cells (panels *d–f*). (*a*) Standard single-molecule fluorescence in situ hybridization (smFISH) uses 20-mer DNA probes with an amine-coupled fluorescent dye to target an mRNA of interest. (*b*) Branched DNA (bDNA) probes increase the multiplicity of fluorophore conjugation by having a homology sequence to both the mRNA and a common sequence on the probe. bDNA probes along with improved tissue clearing techniques have increased intensity to where smFISH can be performed on whole-mount tissues. (*c*) Sequential hybridization enables subsequent rounds of FISH to be performed within the same sample. The results of each round, through the use of barcoding techniques based on a simple Hamming code, can be aggregated to form a unique signature for many RNAs within the same cell. (*d*) Molecular beacons (MBs) offer reduced background by turning on fluorescence after target hybridization. Complex and nonuniform loading techniques limit MBs' application to image endogenous transcripts. (*e*) Spinach-based RNA aptamers form a secondary structure compatible with conditionally fluorescent dyes, activated upon binding. (*f*) Stem-loop labeling using MS2, PP7, or other derivatives gives robust signal intensity for single-molecule tracking of mRNA. Extensive engineering of the stem-loop systems has allowed for live-cell study of all facets of the life of a transcript from transcription through degradation.

equally perturbative method, which limits MB application. Most recently, RNA-targeting, fluorescently labeled dCas9 (catalytically inactive Cas9) molecules have been used to visualize endogenous mRNAs in human cells (95), but, to date, this method lacks definitive single-molecule resolution.

Genetically encoded RNA aptamers have significantly improved the ability to detect and track mRNAs in living cells. Aptamers have been engineered to bind to fluorogenic dyes (**Figure 1*e***). Spinach and its subsequent improvements Spinach2 (126), Broccoli (42), and RNA-Mango (35) function like a fluorescent protein by conditionally generating a chromophore but still do not have adequate intensity for single-molecule visualization. Recently, Spinach arrays have shown promise in providing the multivalent signal necessary for single-molecule imaging (151).

The bacteriophage-derived MS2 stem-loop, and its complementary MS2 coat protein (MCP), has become the standard in live-cell imaging of single-mRNA molecules (8). A gene of interest tagged with an array of MS2 stem-loops (usually 24) and an MCP–fluorescent protein (MCP–FP) fusion are coexpressed in the same cell (**Figure 1*f***). The MCP–FP binds an MS2 loop as a dimer, and the multivalent fluorescence signal marks the RNA for single-molecule visualization and tracking. Expressing MS2-tagged mRNAs and MCP–FP in bacteria, yeast, insect, and mammalian cells can be achieved through homologous recombination (12, 48, 61, 138), retroviral infection (143), or plasmid transfection (8, 31). A homozygous knock-in mouse expressing an MS2 array in the 3′ untranslated region of the β-actin locus and an MCP–GFP fusion has allowed for visualization of mRNA dynamics of an endogenously expressed gene (75, 98, 148). In combination with the MS2 system, the orthogonal bacteriophage-derived PP7 stem-loop recognition system allows for specific dual-color labeling and simultaneous tracking of multiple RNA species in a single cell (19, 61, 74). Moreover, PP7 stem-loops show more complete labeling by PP7 coat protein (PCP) than their MS2 counterpart, improving the signal-to-noise ratio without additional binding sites (69, 142). Other specialized stem-loop and coat-protein labeling systems such as Bgl stem-loops (21), λ boxB RNA (67), and U1A tagging (14, 130) have further expanded the ability to multiplex mRNA tracking in live cells.

Advancements in microscopy have also enabled more sensitive and quantitative measurements of mRNA–protein interactions in vivo using two-photon fluorescence fluctuation spectroscopy (FFS) (141). This technique relies on excitation of a subfemtoliter volume to extract mRNA diffusion information and stoichiometry of interactions between RNA and proteins (142). For instance, measurements of β-actin MCP–MS2–labeled mRNA association with zipcode binding protein 1 (ZBP1) have shown that mRNAs' translatability is spatially controlled (142). Brighter and more stable fluorophores (reviewed in 77 and 108) have also increased the sensitivity of single-mRNA tracking in live cells. HaloTag (79), a genetically encoded label derived from bacterial dehalogenase, can covalently bind bright, photostable, and cell-permeable ligands (49). It offers a significant improvement over intrinsically fluorescent proteins.

Methods in both fixed- and live-cell imaging of individual mRNAs provide a framework to study the biophysics of the mRNA life from transcription through degradation. The following sections discuss recent findings and gene expression models made possible by a spatial understanding of the life of an mRNA.

KINETIC REGULATION OF RNA EXPRESSION FROM BIRTH TO DEATH

The ability to visualize single-mRNA molecules in fixed and living cells enables one to gain spatial and temporal information about gene expression in its natural context. To regulate the phases of gene expression, cells separate different functions into compartments. Isolation is achieved either through membrane separation (e.g., nucleus, mitochondria, lysosome, etc.) or through

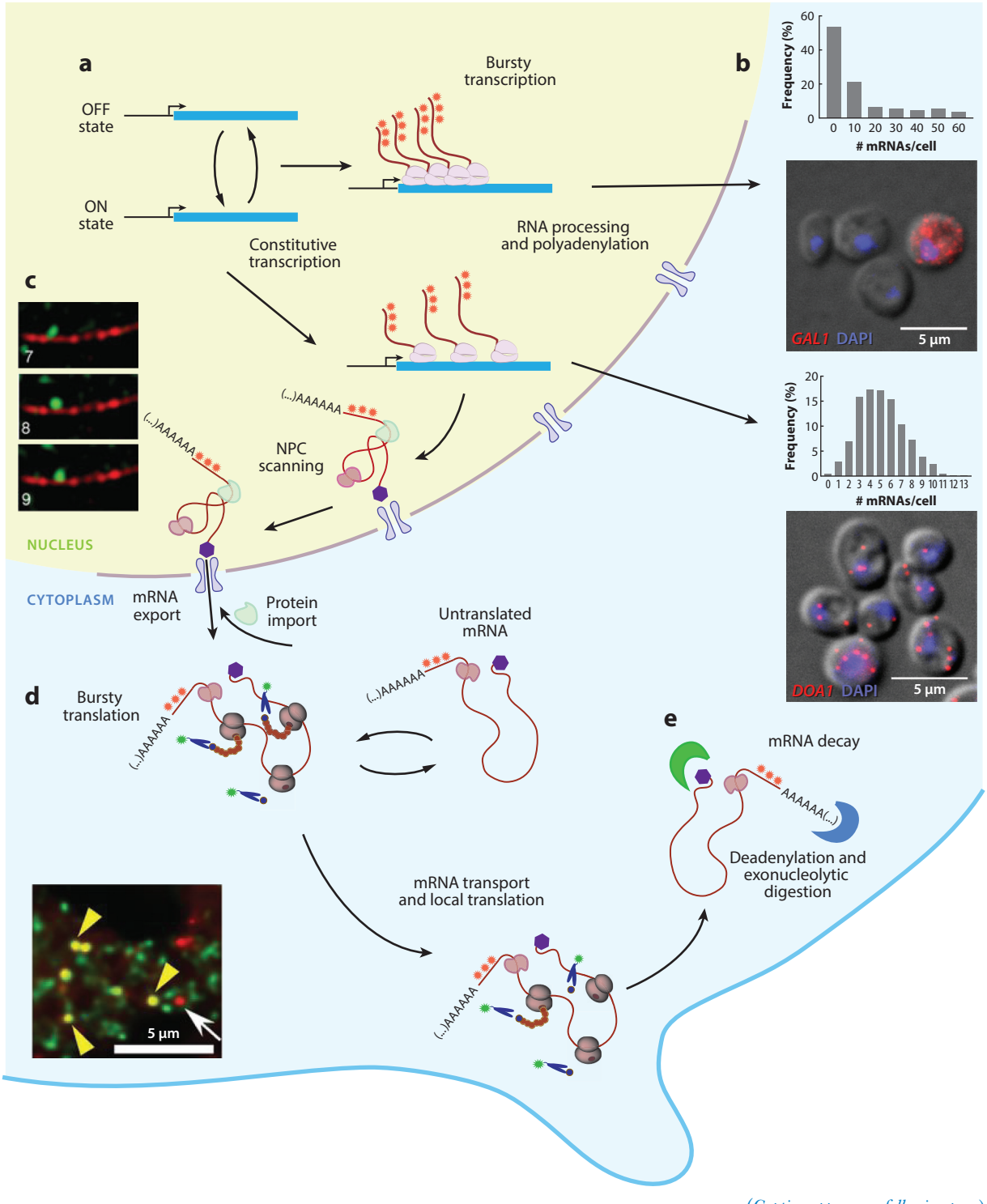

(*Caption appears on following page*)

Figure 2 (*Figure appears on preceding page*)

Following RNAs form birth to death using single-molecule RNA detection methods. Gene expression begins with transcription of RNAs (panels *a* and *b*). Bursty transcription occurs when the gene transitions between the ON and OFF state with a measureable probability, and during the ON state, multiple initiation events take place, followed by periods of inactivity. Constitutive transcription characterizes genes always in the ON state, with constant initiation rate. By using (*a*) the MS2 system in living cells or (*b*) single-molecule fluorescence in situ hybridization (smFISH) in fixed cells, the mode of transcription of a gene is inferred. (*b*, *top*) Example of bursty gene expression: *GAL1* smFISH in *Saccharomyces cerevisiae* shifted from a glucose- to a galactose-containing medium for 2 h. Upon *GAL1* gene induction, less than 10% of the cells express the *GAL1* messenger RNA (mRNA), the number of mRNAs per cell is described by a geometric distribution. (*b*, *bottom*) Example of constitutive gene expression: *DOA1* smFISH in *S. cerevisiae*. All cells express the *DOA1* mRNA, and the number of mRNAs per cell is fitted by a Poisson distribution. smFISH = red; DAPI (4′, 6-diamidino-2-phenylindole stain) = blue (E. Tutucci, unpublished data; smFISH for *GAL1* and *DOA1* were performed as in Reference 138). During transcription, the RNA is processed and polyadenylated. (*c*) Simultaneous imaging of the β-actin mRNA with the MS2 system (*green*) and the nuclear pore complexes (NPCs) (POM121; *red*) (adapted from Reference 50 with permission). The export-competent mRNP scans the nuclear pore before being exported into the cytoplasm. (*d*) Once exported, mRNAs either are translated in the cytoplasm or are localized to specific subcompartments where their translation is regulated. Visualization of single mRNA translation was achieved by combining the MS2 system to visualize the mRNA (*red*) with the SunTag system to visualize the nascent peptide (*green*). Translated mRNAs appear as yellow spots (*yellow arrows*), while untranslated mRNAs appear as red spots (*white arrow*). Image in panel *d* adapted from Reference 143 with permission. (*e*) Decay is the latest step of the mRNA life and the ultimate step controlling the available amount of mRNA in the cell. Recent improvements of the MS2 system led to the development of a reporter system that can be used to faithfully report the life of unstable mRNA, such as cell-cycle mRNAs in *S. cerevisiae*.

membraneless structures [e.g., the nucleolus, Cajal bodies, P-bodies (processing bodies), stress granules, P granules (*Caenorhabditis elegans* germ granules), etc.] (118). In its journey from the transcription site to the cytoplasm, mRNA interacts successively with different compartments, each associated with various RNA binding proteins, forming the mRNPs. The dynamic exchange of the mRNP wardrobe occurs during mRNA processing, export, translation, and decay, suggesting a tight interconnection among all steps (51, 120, 137). In this section, we focus on what single-mRNA molecule imaging studies tell us about these major steps in the life of mRNA.

Transcription Initiation

Cells continuously adapt the transcriptional program in response to changes in cellular needs. In this process, transcription factors (TFs) act as a cellular sensor that interprets variations in the environment and controls transcription by binding to specific DNA sequences on promoters. By using single TF tracking methods, several studies demonstrated that TF density, chromatin structure, and higher-order nuclear architecture influence the search of TF binding sites (reviewed in 20, 92, and 136). Kinetic studies showed that TF binding, such as p53 or the glucocorticoid receptor, is very transient (a few seconds on the DNA), with only a small fraction of TF engaged in productive binding (~8%) (90). These transient interactions only infrequently establish the transcriptional preinitiation complex (PIC), explaining why only 13% of the time RNA polymerase II (RNAPII) binding leads to transcription elongation (125). smFISH or live-imaging measurements of nascent RNAs revealed that genes can have different modes of transcription. Transcription initiation can be described by either a one-state or a two-state model (**Figure 2*a*,*b***) (61, 69, 75, 106). The one-state model describes genes transcribed with a constant initiation rate and nascent transcript number described by a Poisson distribution (45, 150). In contrast, the two-state model describes so-called bursty genes that stochastically switch between an active and inactive state. The nascent and mature RNAs produced by bursty genes are highly variable in a cell population (4, 28, 109). The measured histogram can be fitted to a negative binomial distribution (11, 23, 44, 48, 69, 104, 113, 128, 150), and the dynamic parameters can be extracted from the fitting. The number of nascent RNAs produced during the active state is called burst size, while the rate of switching between

states is defined as burst frequency. In eukaryotes and prokaryotes, transcription is predominantly bursty, but all genes seem to be characterized by different bursting properties, making transcriptional modeling very difficult. Both the frequency and amplitude of bursts can be modulated, leading to expression heterogeneity. The implications of gene expression variability, or so-called noise, are further discussed in the section titled Single-Cell Analysis: Noise in Gene Expression.

To date, the underlying causes of transcriptional bursting remain to be elucidated. Several nonmutually exclusive mechanisms have been proposed to explain the phenomena (71). In bacteria, during transcription by RNAPII, positive supercoiling builds up behind the polymerases, inducing a slowdown of transcription elongation and initiation (23). The action of DNA gyrases, which are limiting in *Escherichia coli*, relieves the supercoiling and allows transcription to restart with a new burst. In *Saccharomyces cerevisiae*, genes are transcribed with either constitutive or bursty modes of transcription (150). Comparison between these classes of genes revealed that the promoter architecture and chromatin remodeling are important. Bursty genes, such as the *GAL* gene cluster, have a TATA box in their promoter, and they are regulated by the SAGA (Spt-Ada-Gcn5-acetyltransferase) transcriptional complex (**Figure 2*b***) (45, 70). It was previously shown in yeast that *cis* elements like AT-rich content can affect nucleosome positioning (63), which in turn could regulate access to TF. Modulation of transcription factor binding can ultimately affect kinetics of transcription initiation in yeast (55, 107). In *Drosophila*, the enhancers' positon, strength, and interactions with promoters govern burst characteristics, changing the probability of a gene being active (44). Finally, in mammalian cells, gene bursting seems to be regulated by a combination of mechanisms, including chromosomal location, chromatin environment, or TF concentration (28, 68, 113, 125). Interestingly, Tantale et al. (133) recently showed using the MS2 system in mammalian cells that transcriptional bursts are generated by groups of closely spaced polymerase convoys. In addition, they showed that bursting can occur on different timescales and that short bursts (i.e., lasting minutes) are controlled by the key transcriptional activator Mediator, while long bursts (i.e., lasting hours) are controlled by the TATA-binding protein. These studies suggest that multiple ways exist to modulate transcription initiation, all relying on highly transient and dynamic interactions. Additional single-molecule studies are required for deciphering the mechanism modulating this process.

Transcription Elongation and Cotranscriptional Processing

The assembly of the PIC at promoters leads to the recruitment and positioning of the RNA polymerases at the transcription start site. This process triggers the synthesis of RNA, a process called elongation. To study the dynamics of transcription, fluorescence recovery after photobleaching (FRAP) of fluorescently labeled RNA polymerases or nascent RNAs has been extensively used in living cells (31, 36, 125). This revealed that the release efficiency of RNAPII from the promoter region to start elongation, promoter escape, is highly variable (31, 125, 152). It has been recently proposed that the chromatin state influences promoter escape rates and that histone hypoacetylation correlates with low escape efficiency (<10%), while hyperacetylation correlates with higher efficiency (>90%) but also with higher variability (31, 125, 152). Live imaging was used to measure the elongation rate of RNA polymerases, with variable results (71). In bacteria, transcription of a reporter gene tagged with the MS2 system was estimated to be 1.5 kb/min (48). In mammalian cells, RNAPII was reported to move at approximately 4 kb/min (31, 133). Measurements performed in *S. cerevisiae* showed that the elongation rate of its longest gene, *MDN1* (14.7 kb), can be highly variable, going from 1 to 4 kb/min (61, 69). These studies suggest that RNAPII elongation may be less processive than previously thought and may be influenced by the chromatin state or by cotranscriptional events involved in RNA processing leading to frequent RNAPII pausing.

The causes of RNAPII pausing are unclear, but they may be linked to cotranscriptional RNA processing, including 5′ RNA capping, splicing, 3′ RNA cleavage, and polyadenylation (2). Recent studies used single-RNA imaging approaches in living human cells to infer the kinetics of cotranscriptional splicing (15, 26, 83, 111). MS2, PP7, or the λB arrays were inserted into the intronic sequences of splicing reporters to measure (by FFS) the time spent by the intron at the transcription site. These studies concluded that intron splicing takes 20–267 s after transcription of the 3′ splice site. The variability of the reported measurements is possibly due to the different type of imaging analysis used in these studies and differences in splicing reporters (3′ cleavage and polyadenylation sites) that can change the residence time of the nascent RNA at the transcription site and affect the splicing measurements. A causal link between splicing kinetics and transcription elongation remains to be established.

Finally, before its release from the transcription site, the mRNA is endonucleolytically cleaved and polyadenylated (120). Completion of this step regulates nuclear export and mRNA localization, translation, and decay. Live imaging of the dwell time of the mRNAs at the transcription site after elongation estimated that 3′-end processing takes between 70 and 100 s to complete (69, 133). Further work may elucidate whether the kinetics of transcription elongation and 3′-end processing are linked to the widespread phenomenon of alternative polyadenylation.

mRNA Export to the Cytoplasm

The formation of export-competent mRNAs starts with the cotranscriptional recruitment of the export machinery. The general mRNA export receptor NXF1 (Mex67 in yeast) interacts with members of the transcription-coupled complex (THO/TREX) and the exon junction complex deposited during splicing to transport the mRNAs through the nuclear pore complexes (NPCs) (59, 137). On the basis of quantification of the number of transcribed mRNAs (2,000–3,000) and the number of nuclear pores present in the nuclear envelope of *S. cerevisiae* (50–200), it was estimated that each nuclear pore transports on average 10–50 mRNAs per min (59). Diffusion of the mRNPs in the nucleoplasm brings them to the nuclear periphery, where they scan multiple NPCs before reaching the cytoplasm (50, 88, 110, 119, 122, 123). mRNA-export visualization in yeast and mammalian cells using the MS2/PP7 systems revealed that mRNAs take 200–500 ms to cross the nuclear membrane (**Figure 2*b***) (50, 88, 122). Based on the kinetic analysis of mRNP export, the current three-step model encompasses the following phases: docking (80 ms), transport (5–20 ms), and release in the cytoplasm (80 ms) (50). This model suggests that two steps of mRNP remodeling may occur on the nuclear and cytoplasmic sides of the NPC (**Figure 2*c***). The delay of the mRNP on the nuclear side could reflect quality-control steps checking whether the mRNA is correctly spliced and processed. The delay on the cytoplasmic side of the NPC is proposed to be caused by the remodeling of the mRNPs and dissociation of the export factors that are recycled in the nucleus (59, 119, 137). Interestingly, it was observed that not all NPCs are available for transport (50, 110), suggesting that mRNP export may be hindered by concomitant bidirectional protein transport. Further work is required to extend these observations to other mRNAs to understand how the size of the mRNP influences export and how a putative quality-control mechanism could recognize mRNAs that are not export competent. Export of mRNAs in the cytoplasm may not exclusively occur through the NPCs. Experiments performed in *Drosophila* suggested that large mRNP cargos can exit the nucleus by budding off the nuclear envelope (124). The mechanisms and the selectivity of this pathway have yet to be elucidated.

Even though kinetic studies suggest that mRNA export is not a rate-limiting step during gene expression, recent investigations propose that this stage can be regulated (3, 6). By using a combination of smFISH and deep sequencing analysis of hundreds of mammalian mRNAs present in the nuclear versus cytoplasmic fractions, these studies suggested that mRNAs can be retained in

the nucleus to buffer transcription variability. Although an intriguing possibility, no mechanism has been presented to explain how mRNA export could actively compensate for the stochastic expression of every mRNA.

mRNA Translation

Once in the cytoplasm, mRNAs can localize to specific cellular compartments where they are locally translated or they can freely diffuse in the cytoplasm to rapidly engage in translation. mRNA localization is a widespread mechanism to control protein expression in space and time, from prokaryotic to eukaryotic cells (reviewed in 16). The possibility of visualizing the mRNAs in intact cells, fixed or live, was essential to discover localization and to hypothesize its role in protein synthesis organization (8, 16, 148), but it wasn't until recently that we could simultaneously visualize single mRNAs and their translational state.

Translating RNA imaging by coat-protein knockoff (TRICK) distinguishes untranslated mRNA from transcripts that have already gone through the pioneer round of translation (54). This reporter was successfully used to study the translation state of the *oskar* mRNA during *Drosophila* development and to confirm that the mRNA is translationally repressed until its localization to the posterior pole. TRICK detects only the pioneer round of translation, but Katz et al. (65) developed an approach that could be used to deduce the translation state of single fluorescent mRNA at any given time. Comovement of MS2-labeled β-actin mRNAs and the 60S large ribosome subunit (L10A) was analyzed in mouse fibroblasts. Single-particle tracking analysis revealed that β-actin mRNA translation mainly occurs at the leading edge of a migrating cell, near the focal adhesion complex. In addition, ribosome-associated translating mRNAs move slower and in a more corralled manner than untranslated mRNAs. Further analysis revealed that individual ribosome-associated β-actin mRNAs can switch between slower and faster diffusing states, implying variability in the translation rate, as previously observed for transcription.

A fundamental improvement came with the development of imaging approaches allowing visualization of nascent peptides produced by single mRNAs tagged with the MS2/PP7 systems (89, 140, 143, 146). To image single proteins with a multivalent tag, the SunTag system (131) attaches multiple fluorescently labeled antibodies to an array of epitopes added to a protein of interest (**Figure 2*d***). Because the antibodies are already mature FPs, an N-terminal SunTag addition can rapidly label nascent peptides at the ribosome exit channel, making a single-molecule readout of translation possible (140, 143, 146). Two seminal papers demonstrated that translation initiation is a stochastic process occurring in bursts, similar to transcription (89, 143). The switching between the active and inactive state can occur in a range between 15 min and 3 h (burst frequency). On actively translating reporters, ribosomes initiate protein synthesis every 30–40 s (burst size), traveling at a distance of 200–300 nucleotides and with an elongation rate of 3–10 amino acids/s. Finally, the use of the single-molecule imaging of nascent peptides (SINAPs) reporter described in Reference 143 directly demonstrated that mRNA localization influences translation rates. Live imaging of single-mRNA translation in neuronal dendrites shows that the percentage of translating mRNAs decreases with the distance from the soma (proximal $\approx$ 40%, whereas distal $\approx$ 10%). As observed by Katz et al. (65), the SINAPs reporter confirms that translating mRNAs move slower than untranslating mRNAs; however, it also shows that even localizing mRNAs can be actively translated while traveling. Thanks to improving genome editing technology, it was recently shown that a SINAPs-like approach can be used to image translation of an endogenously tagged POLR2A mRNA in human cell lines (103). Interestingly, these novel approaches could be used to elucidate the coordination between RNA localization and local translation. The current view suggests that local RNA translation is mainly regulated by the localization of RNA at specific

cellular compartments. However, it was recently shown in intestinal cells that stimulation induced by feeding can lead to apical localization of the mRNAs encoding the translational machinery (87). The local production of ribosomes boosts the translation of apically localized mRNAs favoring nutrient absorption (87). These studies suggest that cells evolved multiple approaches to control polarized translation.

mRNA Decay

To precisely control gene expression, all eukaryotic and prokaryotic cells actively regulate the degradation of RNAs. RNA degradation destroys both RNAs that have reached the end of their useful life and defective RNAs that are recognized by surveillance mechanisms (**Figure 2*e***). More broadly, degradation can be used by cells to counteract transcription to precisely control mRNA levels. Cytoplasmic mRNA degradation is a multistep process, initiated by the deadenylation of the mRNA followed by 3′-to-5′ or 5′-to-3′ exonucleolytic degradation. More frequently, the mRNAs are decapped and degraded via the 5′-to-3′ decay exonuclease Xrn1 (99). Multiple factors influence the half-life of an mRNA. Increasing the length of the 3′ UTR (untranslated region) and mutations in AT-rich sequences both correlate with destabilization of transcripts, possibly due to changes in 3′-end processing and polyadenylation and recruitment of decay factors (102). In addition, the codon optimality and the presence of proteins or microRNA binding sites influence mRNA stability (58). Besides *cis*-regulatory elements, like the mRNA sequence, other components working in *trans*, such as the promoter, regulate the stability of an mRNA (13, 134). Studies performed in yeast showed by smFISH that cell-cycle mRNAs undergo a switch in mRNA stability that induces their rapid degradation (134). The information controlling decay of these mRNAs is encoded by the promoter, but to date, the signal remains elusive. The current model suggests that cotranscriptional recruitment of posttranslational modifiers (kinases, methyltransferases) leads to remodeling of the mRNPs, marking them for rapid degradation in the cytoplasm (51, 85). The process of degradation is tightly coupled to translation, and the decay machinery is proposed to directly compete to access the mRNAs cotranslationally (101). The coordination between translation and decay is particularly important for the identification of mRNAs containing premature termination codons (PTC), the signal triggering nonsense-mediated decay (NMD) (64). Live imaging of a PTC-containing reporter revealed that mutated RNAs are identified cotranscriptionally, possibly by NMD factors (32). This quality-control step is proposed to mark the RNA for rapid degradation, usually occurring within seconds from the export in the cytoplasm (135).

These initial studies have motivated the development of tools aimed at studying mRNA degradation in intact cells. The MS2 labeling system has been broadly applied to study all facets of the mRNA life cycle from transcription to mRNA trafficking to translation (97). This extensive use requires rigorous characterization of aberrations from canonical behavior of an unaltered transcript. System optimization has become especially important in using MS2 to study degradation of transient mRNAs. MCP binding to MS2 loops has been shown to delay 5′-to-3′ degradation under normal and stress conditions in yeast (47, 52, 60), leading to accumulation of MCP-bound MS2 loops misidentified as nondegraded transcripts. Recent optimization of the MS2 system allowed for more accurate visualization of the complete life cycle of unstable cell-cycle mRNAs in yeast, either in normal growing conditions or upon stress (138). The substitution of a single nucleotide in the MS2 loop structure reduced MCP affinity to a point where it no longer affects decay or labeling efficiency (138). In an effort to increase our understanding of mRNA decay in mammalian cells, Chao and colleagues (62) recently described a novel MS2-based reporter system that can measure degradation kinetics in both fixed and live samples. These technologies will be valuable to extend our understanding of mRNA degradation regulation.

QUANTITATIVE MODELS FOR GENE EXPRESSION

The number of mRNAs and proteins is often modeled as a birth–death Markov process. The production of an mRNA or a protein is described by a coupled master equation with one or more rate-limiting steps (**Figure 3*a***) (100). The detailed transcription and translation process is not taken into account and is modeled as a simple rate equation. Transcription and translation are

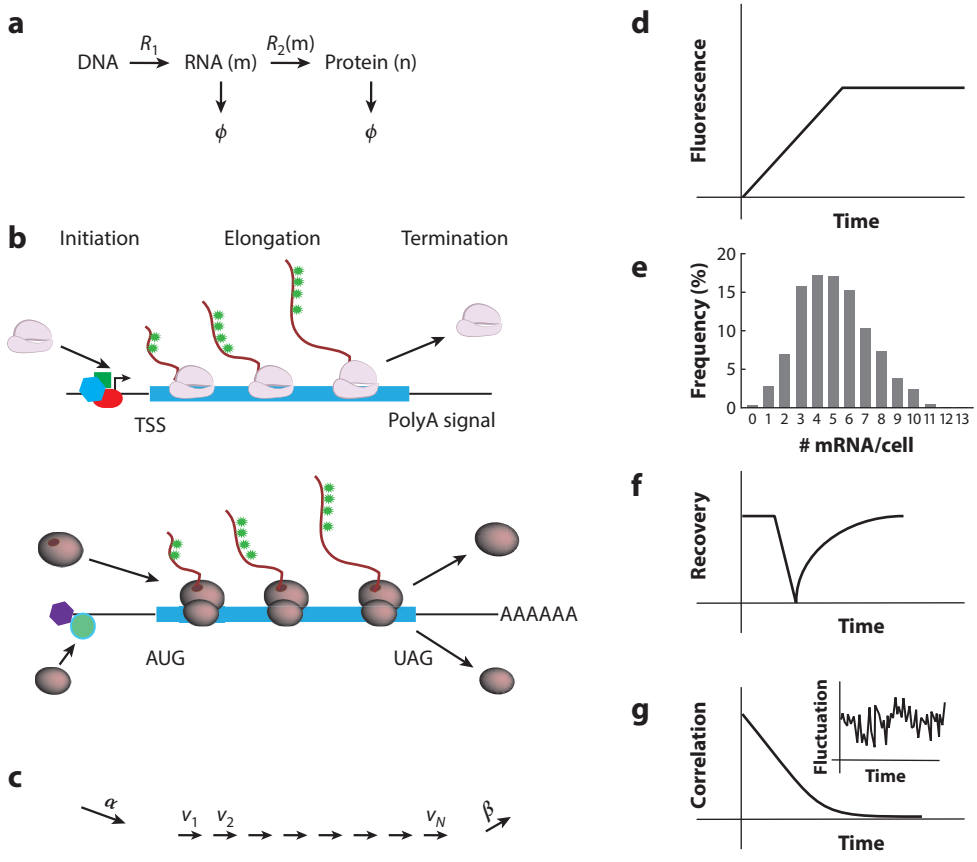

Figure 3

Quantitative model for transcription and translation. (*a*) The generative model for central dogma. The number of messenger RNAs (mRNAs) and proteins can be described by a chemical master equation. The rate [R_2(m)] of protein production depends on the number of mRNAs (m) but not vice-versa (R_1) (m and n are the numbers of mRNA and proteins, respectively; Φ is the degraded molecule). (*b*) Both transcription and translation are described by initiation, elongation, and termination processes. The nascent transcripts and peptides can be visualized by MS2- or single-molecule imaging of nascent peptides–like systems, respectively. (*c*) The coarse-grained model of transcription and translation. The template has N sites. The process initiates with probability α, elongates with site-specific probability v, and terminates with probability β. (*d*) The fluorescence intensity profile while a single molecular machinery (polymerase or ribosome) travels through MS2 or SunTag motifs. Collectively, many machineries simultaneously reside on the template. (*e*) Statistical analysis is required to extract biophysical parameters from the histograms of fluorescence intensity. (*f*) Single-molecule fluorescence recovery after photobleaching (FRAP) or (*g*) correlation analysis of the transcription or translation sites recovers the dynamic information of initiation and elongation. To extract a biophysical model from a FRAP curve or correlation function, one needs to solve the quantitative model shown in panel *c*. Additional abbreviations: PolyA, polyadenylation; TSS, transcription start site.

two essential but distinct phases to express a gene. They are carried out by different machineries, happen in different subcellular compartments, and are regulated by different factors. Despite these differences, there are strong similarities from a biophysical point of view (**Figure 3*b***): A molecular machine travels along a template with defined polarity and synthesizes a biopolymer by adding building blocks one at a time. In addition, both processes are divided into initiation, elongation, and termination stages. There are sophisticated biophysical models to describe each process separately. We believe that the models that describe one process can be applied to the other.

A simple coarse-grained model for both transcription and translation can be described as illustrated in **Figure 3*c***. A polymerase or ribosome travels along a template with N sites. For transcription, N is the total nucleotides of the gene, and for translation, N is the number of codons. The molecular machinery initiates at the start site with a certain probability $\alpha(t)$. For constitutive transcription or translation, the initiation probability is a constant, which means that the waiting time between successive initiation events is exponentially distributed. More often than not, $\alpha(t)$ is time dependent. For a bursting gene, $\alpha(t)$ is modeled as a random telegraph signal in the simplest case. After initiation, the molecule travels along the template with a site-specific probability v_i, which is related to the elongation speed. The assumption here is that the elongation speed depends only on the site and not on its neighbors. For translation, the elongation speed may depend on codon optimality and therefore be site specific. Finally, the molecule leaves the template with a probability β. Throughout this process, the molecule travels only in one direction, and if the next site is occupied, the molecule will not be able to move. In mathematics, this is called a totally asymmetric exclusion process (TASEP) (153). If we further assume that the initiation and elongation speed are both constants, the model has been solved analytically at steady state: The probability of each configuration, the molecular density at each site, the transport flux, and the correlation function between different sites have been calculated (33). Depending on the value of initiation and termination probability, the steady state has been described as three different phases: high density, low density, and maximum current (34). Depending on which step is rate limiting, the molecular density at steady state has a nontrivial distribution along the template. TASEP has been used to model translation and been studied extensively in the literature. Lately, it has been extended to take into account the size of the ribosome (117), pausing because of nonoptimal codons (25), mRNA looping (24), and finite resources of ribosomes (127). Recently, large-scale computational models have been developed using TASEP to describe the production of every mRNA, ribosome, and transfer RNA (tRNA) in a cell (116, 127). From these models, one can infer the rate-limiting steps on the basis of large-scale transcriptome and proteome data. For example, in healthy yeast cells, the protein production is typically limited by the availability of free ribosomes (116). In bacteria, the elongation rate at most codons is not limited by the intracellular concentration of aminoacyl-tRNA but rather by the intraribosomal kinetic events (127). We believe that many mathematical tools from TASEP could also be used to model transcription.

For transcription, the detailed distribution of polymerases, such as the mutual exclusion of polymerase in TASEP, is often not taken into account. This simplified modeling, however, allows one to consider more complicated initiation events. For example, the birth process has often been modeled as bursting owing to DNA supercoiling, promoter architecture, transcription factor binding, or chromatin structure (23, 104, 109, 150). These models give simple explanations for the cell-to-cell heterogeneity revealed in the single-cell fluorescence reporter assay. With smFISH, the distribution of mature and nascent mRNAs has been measured experimentally. Fitting the distribution to a biophysical model leads to measurement of initiation rate, elongation rate, and the bursting frequency (**Figure 3*d*,*e***) (104, 150). Although one can infer a lot of dynamic information from a snapshot of protein and mRNA distribution, it is highly desirable to directly observe the real-time transcription and translation dynamics directly in live cells. As previously

discussed, the MS2/PP7 systems together with SINAPs, FRAP (**Figure 3*f***), and fluctuation analysis (**Figure 3*g***) have been used to measure transcription and translation dynamics. To extract quantitative parameters from these experiments, a biophysical model to describe the dynamic events is needed. TASEP is the first nontrivial coarse-grained model that incorporates the most basic ingredients of the polymerization process. However, the exact expression is cumbersome (153) and the analytical temporal dynamics are still not available. Currently, the transition probability between sites is approximated as a simple rate equation (31, 69), which leads to the analytical equation for the fluorescence recovery or autocorrelation function. The approximation will break down when the rate of transcription or translation is high or there is a traffic jam. Further theoretical work on the exact and approximate solution for TASEP is needed to describe the detailed nascent chain dynamics during transcription and translation.

SINGLE-CELL ANALYSIS: NOISE IN GENE EXPRESSION

During the early steps of animal development, the asymmetric expression of key pluripotency TF controls the differentiation of stem cells to give rise to more than 200 cell types (10, 18, 41, 129). Studies aimed at elucidating how cells establish gene expression asymmetry identified noise, generated by stochastic gene expression, as a major source of mRNA and protein variability (38, 107, 109, 144). Noise in gene expression is defined as the standard deviation divided by the mean of the distribution of mRNAs or protein concentration, and it contains extrinsic and intrinsic components (38). The first component is produced by the fluctuations of the proteins controlling gene expression (i.e., transcription factors, polymerases, ribosomes, etc.), while the second component depends on the stochastic nature of each step during gene expression (i.e., promoter activation, transcription, translation, and mRNA and protein decay) (38). The use of single-cell organisms such as *E. coli* or *S. cerevisiae* enables the quantification of intrinsic and extrinsic noise in isogenic populations. Substantial variability was demonstrated by using fluorescent protein reporters (e.g., CFP and YFP) expressed by two identical alleles (38, 107) or by different promoter variants (55, 56). These studies revealed that noise is gene specific and that unique combinations of regulatory sequences (promoter, enhancers, insulators) and transcriptional regulators (TF expression, frequency, or amplitude) influence the ratio between intrinsic and extrinsic noise and, in turn, the mRNAs and protein levels. In eukaryotic cells, a substantial contribution to variability is attributable to transcriptional bursting (9, 46, 48, 107). smFISH or live-imaging experiments in bacteria, yeast, or mammalian cells were extensively used to estimate the mean and the variance of mRNAs in a population of cells (72, 104, 144, 150). This approach calculates the size and frequency of transcription bursts (48, 69, 104, 121, 145, 150) and found a positive correlation between the burst size and the noise amplitude (45, 104, 113, 114, 128, 150).

Gene expression noise is not restricted to transcription. mRNA translation is also a bursty process that must deal with highly variable amounts of mRNAs (17, 89, 143, 146). Studies performed in budding and fission yeasts revealed that cells express on average between 0 and 1,000 mRNA molecules per cell, per gene (61, 82, 150). In addition, 75% of genes have between 0 and 10 mRNA molecules (61, 150). These observations suggested the possibility that cells could adapt the translation rate to buffer mRNA concentrations (76). Several studies, using a combination of RNA sequencing (RNA-seq) and ribosome profiling, came to suggest that there is no significant compensation at the level of translation rate (1, 7, 94), implying protein-level regulation relies on post-translational mechanisms controlling protein stability (45). Consistent with this view, the absolute quantifications of mRNAs and proteins in mammalian cells by using a combination of RNA-seq and pSILAC (pulsed stable isotope labeling by/with amino acids in cell culture) (112) revealed that the

mRNA levels influence ~84% of the variance in protein levels, while the translation rate controls ~9% of the protein levels (73, 112). Despite the progress obtained in measuring mRNA and protein levels in single cells, a few studies reported the simultaneous quantification of both molecules in the same cells and at a large scale (30, 132). In contrast to the results obtained with global approaches, these studies revealed no correlation between mRNA and protein copy numbers in single cells. The work from Taniguchi et al. (132) simultaneously imaged 137 proteins and mRNAs in *E. coli* and found no significant correlation. One possible explanation for this result is that the mRNAs′ half-life is shorter compared to that of the proteins. However, it is also possible that extrinsic noise during translation, due to translation factor availability or mRNA and protein decay, contributes to variability more than previously considered (27, 29). For instance, localization of mRNAs in discrete compartments can significantly change the probability of mRNAs being translated (16, 87).

The equilibrium between noise reduction and noise amplification is a dynamic process that cells use to guarantee reproducibility of cellular responses and, in contrast, phenotypic diversity to survive in response to stressful conditions. A priority for future research is to develop tools that simultaneously measure mRNA and protein levels in single cells to understand the sources of noise and how they are coordinated to generate consistent phenotypes.

FUTURE DIRECTIONS: GENE EXPRESSION ANALYSIS IN SINGLE CELLS OVER TIME

To understand how rare and dynamic events during gene expression generate reproducible phenotypes, developing methods that follow mRNAs and proteins in single cells over long periods of time is essential. Substantial progress has been made in developing single-cell tools for measuring DNA, RNA, and proteins (37, 143, 149), but we have yet to be able to perform simultaneous in situ transcriptomic and proteomic analysis over several generations and in intact tissue. Current methods of gene expression analysis combined with lineage tracing are mainly performed in fixed cells (43). Even with high resolution, fixed methods remain indirect approaches to study gene expression dynamics. As previously described, RNA labeling methods like the MS2 or the PP7 systems have proven to be efficient for visualizing and quantifying single-mRNA molecules in living cells, but they have been restricted to specific, genetically labeled mRNAs. New methods are needed to label many endogenous mRNAs in living cells, preferably without genetically engineering the cells, so that multiple native mRNAs can be examined simultaneously. Continuous long-term imaging of single-mRNA molecules (for several cell divisions) remains challenging in both living cells and tissues. Several problems limit this kind of approach: limited fluorophore brightness and photostability, phototoxicity and the capability of keeping cells, and tissues and organs in physiological conditions for long periods of time (66, 77). We predict that these limitations represent the future challenges to advancing the field of quantitative biology.

DISCLOSURE STATEMENT

Robert H. Singer and Evelina Tutucci have submitted a provisional application to the US Patent and Trademark Office (no. 62/487,058) for a new MS2 system for the visualization of single mRNA (described in this review and Reference 138). It has not been licensed to any corporation, and the authors (Robert H. Singer, Evelina Tutucci, and Maria Vera) are the sole inventors.

ACKNOWLEDGMENTS

This work was supported by NIH Grant GM57071 to R.H.S. E.T. was supported by Swiss National Science Foundation Fellowships P2GEP3_155692 and P300PA_164717. N.M.L. was supported by NIH Training Grant T32 GM007445.

LITERATURE CITED

1. Albert FW, Muzzey D, Weissman JS, Kruglyak L. 2014. Genetic influences on translation in yeast. *PLOS Genet*. 10:e1004692
2. Alpert T, Herzel L, Neugebauer KM. 2017. Perfect timing: splicing and transcription rates in living cells. *WIREs RNA* 8:e1401
3. Bahar Halpern K, Caspi I, Lemze D, Levy M, Landen S, et al. 2015. Nuclear retention of mRNA in mammalian tissues. *Cell Rep*. 13:2653–62
4. Bahar Halpern K, Tanami S, Landen S, Chapal M, Szlak L, et al. 2015. Bursty gene expression in the intact mammalian liver. *Mol. Cell* 58:147–56
5. Battich N, Stoeger T, Pelkmans L. 2013. Image-based transcriptomics in thousands of single human cells at single-molecule resolution. *Nat. Methods* 10:1127–33
6. Battich N, Stoeger T, Pelkmans L. 2015. Control of transcript variability in single mammalian cells. *Cell* 163:1596–610
7. Battle A, Khan Z, Wang SH, Mitrano A, Ford MJ, et al. 2015. Genomic variation. Impact of regulatory variation from RNA to protein. *Science* 347:664–67
8. Bertrand E, Chartrand P, Schaefer M, Shenoy SM, Singer RH, Long RM. 1998. Localization of ASH1 mRNA particles in living yeast. *Mol. Cell* 2:437–45
9. Blake WJ, KÆrn M, Cantor CR, Collins JJ. 2003. Noise in eukaryotic gene expression. *Nature* 422:633–37
10. Boiani M, Schöler HR. 2005. Regulatory networks in embryo-derived pluripotent stem cells. *Nat. Rev. Mol. Cell Biol.* 6:872–84
11. Bothma JP, Garcia HG, Esposito E, Schlissel G, Gregor T, Levine M. 2014. Dynamic regulation of *eve* stripe 2 expression reveals transcriptional bursts in living *Drosophila* embryos. *PNAS* 111:10598–603
12. Bothma JP, Garcia HG, Ng S, Perry MW, Gregor T, Levine M. 2015. Enhancer additivity and non-additivity are determined by enhancer strength in the *Drosophila* embryo. *eLife* 4:e07956
13. Bregman A, Avraham-Kelbert M, Barkai O, Duek L, Guterman A, Choder M. 2011. Promoter elements regulate cytoplasmic mRNA decay. *Cell* 147:1473–83
14. Brodsky AS, Silver PA. 2002. Identifying proteins that affect mRNA localization in living cells. *Methods* 26:151–55
15. Brody Y, Neufeld N, Bieberstein N, Causse SZ, Bohnlein EM, et al. 2011. The in vivo kinetics of RNA polymerase II elongation during co-transcriptional splicing. *PLOS Biol*. 9:e1000573
16. Buxbaum AR, Haimovich G, Singer RH. 2015. In the right place at the right time: visualizing and understanding mRNA localization. *Nat. Rev. Mol. Cell Biol.* 16:95–109
17. Cai L, Friedman N, Xie XS. 2006. Stochastic protein expression in individual cells at the single molecule level. *Nature* 440:358–62
18. Chambers I, Silva J, Colby D, Nichols J, Nijmeijer B, et al. 2007. Nanog safeguards pluripotency and mediates germline development. *Nature* 450:1230–34
19. Chao JA, Patskovsky Y, Almo SC, Singer RH. 2008. Structural basis for the coevolution of a viral RNA–protein complex. *Nat. Struct. Mol. Biol.* 15:103–5
20. Chen H, Larson DR. 2016. What have single-molecule studies taught us about gene expression? *Genes Dev*. 30:1796–810
21. Chen J, Nikolaitchik O, Singh J, Wright A, Bencsics CE, et al. 2009. High efficiency of HIV-1 genomic RNA packaging and heterozygote formation revealed by single virion analysis. *PNAS* 106:13535–40
22. Chen KH, Boettiger AN, Moffitt JR, Wang S, Zhuang X. 2015. RNA imaging. Spatially resolved, highly multiplexed RNA profiling in single cells. *Science* 348:aaa6090

23. Chong S, Chen C, Ge H, Xie XS. 2014. Mechanism of transcriptional bursting in bacteria. *Cell* 158:314–26
24. Chou T. 2003. Ribosome recycling, diffusion, and mRNA loop formation in translational regulation. *Biophys. J.* 85:755–73
25. Chou T, Lakatos G. 2004. Clustered bottlenecks in mRNA translation and protein synthesis. *Phys. Rev. Lett.* 93:198101
26. Coulon A, Ferguson ML, de Turris V, Palangat M, Chow CC, Larson DR. 2014. Kinetic competition during the transcription cycle results in stochastic RNA processing. *eLife* 3:e03939
27. Dacheux E, Malys N, Meng X, Ramachandran V, Mendes P, McCarthy JEG. 2017. Translation initiation events on structured eukaryotic mRNAs generate gene expression noise. *Nucleic Acids Res.* 45:6981–92
28. Dar RD, Razooky BS, Singh A, Trimeloni TV, McCollum JM, et al. 2012. Transcriptional burst frequency and burst size are equally modulated across the human genome. *PNAS* 109:17454–59
29. Dar RD, Razooky BS, Weinberger LS, Cox CD, Simpson ML. 2015. The low noise limit in gene expression. *PLOS ONE* 10:e0140969
30. Darmanis S, Gallant CJ, Marinescu VD, Niklasson M, Segerman A, et al. 2016. Simultaneous multiplexed measurement of RNA and proteins in single cells. *Cell Rep.* 14:380–89
31. Darzacq X, Shav-Tal Y, de Turris V, Brody Y, Shenoy SM, et al. 2007. In vivo dynamics of RNA polymerase II transcription. *Nat. Struct. Mol. Biol.* 14:796–806
32. de Turris V, Nicholson P, Orozco RZ, Singer RH, Muhlemann O. 2011. Cotranscriptional effect of a premature termination codon revealed by live-cell imaging. *RNA* 17:2094–107
33. Derrida B. 1998. An exactly soluble non-equilibrium system: the asymmetric simple exclusion process. *Phys. Rep.* 301:65–83
34. Derrida B, Domany E, Mukamel D. 1992. An exact solution of a one-dimensional asymmetric exclusion model with open boundaries. *J. Stat. Phys.* 69:667–87
35. Dolgosheina EV, Jeng SCY, Panchapakesan SSS, Cojocaru R, Chen PSK, et al. 2014. RNA Mango aptamer-fluorophore: a bright, high-affinity complex for RNA labeling and tracking. *ACS Chem. Biol.* 9:2412–20
36. Dundr M, Hoffmann-Rohrer U, Hu Q, Grummt I, Rothblum LI, et al. 2002. A kinetic framework for a mammalian RNA polymerase in vivo. *Science* 298:1623–26
37. Eliscovich C, Shenoy SM, Singer RH. 2017. Imaging mRNA and protein interactions within neurons. *PNAS* 114:E1875–84
38. Elowitz MB, Levine AJ, Siggia ED, Swain PS. 2002. Stochastic gene expression in a single cell. *Science* 297:1183–86
39. Femino AM, Fay FS, Fogarty K, Singer RH. 1998. Visualization of single RNA transcripts in situ. *Science* 280:585–90
40. Femino AM, Fogarty K, Lifshitz LM, Carrington W, Singer RH. 2003. Visualization of single molecules of mRNA in situ. *Methods Enzymol.* 361:245–304
41. Filipczyk A, Marr C, Hastreiter S, Feigelman J, Schwarzfischer M, et al. 2015. Network plasticity of pluripotency transcription factors in embryonic stem cells. *Nat. Cell Biol.* 17:1235–46
42. Filonov GS, Moon JD, Svensen N, Jaffrey SR. 2014. Broccoli: rapid selection of an RNA mimic of green fluorescent protein by fluorescence-based selection and directed evolution. *J. Am. Chem. Soc.* 136:16299–308
43. Frieda KL, Linton JM, Hormoz S, Choi J, Chow K-HK, et al. 2017. Synthetic recording and in situ readout of lineage information in single cells. *Nature* 541:107–11
44. Fukaya T, Lim B, Levine M. 2016. Enhancer control of transcriptional bursting. *Cell* 166:358–68
45. Gandhi SJ, Zenklusen D, Lionnet T, Singer RH. 2011. Transcription of functionally related constitutive genes is not coordinated. *Nat. Struct. Mol. Biol.* 18:27–34
46. Garcia HG, Tikhonov M, Lin A, Gregor T. 2013. Quantitative imaging of transcription in living *Drosophila* embryos links polymerase activity to patterning. *Curr. Biol.* 23:2140–45
47. Garcia JF, Parker R. 2015. MS2 coat proteins bound to yeast mRNAs block 5′ to 3′ degradation and trap mRNA decay products: implications for the localization of mRNAs by MS2-MCP system. *RNA* 21:1393–95

48. Golding I, Paulsson J, Zawilski SM, Cox EC. 2005. Real-time kinetics of gene activity in individual bacteria. *Cell* 123:1025–36
49. Grimm JB, English BP, Choi H, Muthusamy AK, Mehl BP, et al. 2016. Bright photoactivatable fluorophores for single-molecule imaging. *Nat. Methods* 13:985–88
50. Grunwald D, Singer RH. 2010. In vivo imaging of labelled endogenous β-actin mRNA during nucleocytoplasmic transport. *Nature* 467:604–7
51. Haimovich G, Choder M, Singer RH, Trcek T. 2013. The fate of the messenger is pre-determined: a new model for regulation of gene expression. *Biochim. Biophys. Acta* 1829:643–53
52. Haimovich G, Zabezhinsky D, Haas B, Slobodin B, Purushothaman P, et al. 2016. Use of the MS2 aptamer and coat protein for RNA localization in yeast: a response to "MS2 coat proteins bound to yeast mRNAs block 5′ to 3′ degradation and trap mRNA decay products: implications for the localization of mRNAs by MS2-MCP system." *RNA* 22:660–66
53. Halpern KB, Shenhav R, Matcovitch-Natan O, Toth B, Lemze D, et al. 2017. Single-cell spatial reconstruction reveals global division of labour in the mammalian liver. *Nature* 542:352–56
54. Halstead JM, Lionnet T, Wilbertz JH, Wippich F, Ephrussi A, et al. 2015. An RNA biosensor for imaging the first round of translation from single cells to living animals. *Science* 347:1367–671
55. Hansen AS, O'Shea EK. 2013. Promoter decoding of transcription factor dynamics involves a trade-off between noise and control of gene expression. *Mol. Syst. Biol.* 9:704
56. Hansen AS, O'Shea EK. 2015. Limits on information transduction through amplitude and frequency regulation of transcription factor activity. *eLife* 4:e06559
57. Hansen CH, van Oudenaarden A. 2013. Allele-specific detection of single mRNA molecules in situ. *Nat. Methods* 10:869–71
58. Hanson G, Coller J. 2018. Codon optimality, bias and usage in translation and mRNA decay. *Nat Rev Mol. Cell Biol.* 19:20–30
59. Heinrich S, Derrer CP, Lari A, Weis K, Montpetit B. 2017. Temporal and spatial regulation of mRNA export: Single particle RNA-imaging provides new tools and insights. *BioEssays* 39:1600124
60. Heinrich S, Sidler CL, Azzalin CM, Weis K. 2017. Stem-loop RNA labeling can affect nuclear and cytoplasmic mRNA processing. *RNA* 23:134–41
61. Hocine S, Raymond P, Zenklusen D, Chao JA, Singer RH. 2013. Single-molecule analysis of gene expression using two-color RNA labeling in live yeast. *Nat. Methods* 10:119–21
62. Horvathova I, Voigt F, Kotrys AV, Zhan Y, Artus-Revel CG, et al. 2017. The dynamics of mRNA turnover revealed by single-molecule imaging in single cells. *Mol. Cell* 68:615–25.e9
63. Jansen A, Verstrepen KJ. 2011. Nucleosome positioning in *Saccharomyces cerevisiae*. *Microbiol. Mol. Biol. Rev*. 75:301–20
64. Karousis ED, Nasif S, Mühlemann O. 2016. Nonsense-mediated mRNA decay: novel mechanistic insights and biological impact. *WIREs RNA* 7:661–82
65. Katz ZB, English BP, Lionnet T, Yoon YJ, Monnier N, et al. 2016. Mapping translation 'hot-spots' in live cells by tracking single molecules of mRNA and ribosomes. *eLife* 5:e10415
66. Laissue PP, Alghamdi RA, Tomancak P, Reynaud EG, Shroff H. 2017. Assessing phototoxicity in live fluorescence imaging. *Nat. Methods* 14:657–61
67. Lange S, Katayama Y, Schmid M, Burkacky O, Brauchle C, et al. 2008. Simultaneous transport of different localized mRNA species revealed by live-cell imaging. *Traffic* 9:1256–67
68. Larson DR, Fritzsch C, Sun L, Meng X, Lawrence DS, Singer RH. 2013. Direct observation of frequency modulated transcription in single cells using light activation. *eLife* 2:e00750
69. Larson DR, Zenklusen D, Wu B, Chao JA, Singer RH. 2011. Real-time observation of transcription initiation and elongation on an endogenous yeast gene. *Science* 332:475–78
70. Lenstra TL, Coulon A, Chow CC, Larson DR. 2015. Single-molecule imaging reveals a switch between spurious and functional ncRNA transcription. *Mol. Cell* 60:597–610
71. Lenstra TL, Rodriguez J, Chen H, Larson DR. 2016. Transcription dynamics in living cells. *Annu. Rev. Biophys.* 45:25–47

72. Levsky JM, Shenoy SM, Pezo RC, Singer RH. 2002. Single-cell gene expression profiling. *Science* 297:836–40
73. Li JJ, Bickel PJ, Biggin MD. 2014. System wide analyses have underestimated protein abundances and the importance of transcription in mammals. *PeerJ* 2:e270
74. Lim F, Downey TP, Peabody DS. 2001. Translational repression and specific RNA binding by the coat protein of the *Pseudomonas* phage PP7. *J. Biol. Chem.* 276:22507–13
75. Lionnet T, Czaplinski K, Darzacq X, Shav-Tal Y, Wells AL, et al. 2011. A transgenic mouse for in vivo detection of endogenous labeled mRNA. *Nat. Methods* 8:165–70
76. Liu Y, Beyer A, Aebersold R. 2016. On the dependency of cellular protein levels on mRNA abundance. *Cell* 165:535–50
77. Liu Z, Lavis LD, Betzig E. 2015. Imaging live-cell dynamics and structure at the single-molecule level. *Mol. Cell* 58:644–59
78. Long X, Colonell J, Wong AM, Singer RH, Lionnet T. 2017. Quantitative mRNA imaging throughout the entire *Drosophila* brain. *Nat. Methods* 14:703–6
79. Los GV, Encell LP, McDougall MG, Hartzell DD, Karassina N, et al. 2008. HaloTag: a novel protein labeling technology for cell imaging and protein analysis. *ACS Chem. Biol.* 3:373–82
80. Lubeck E, Cai L. 2012. Single-cell systems biology by super-resolution imaging and combinatorial labeling. *Nat. Methods* 9:743–48
81. Lubeck E, Coskun AF, Zhiyentayev T, Ahmad M, Cai L. 2014. Single-cell in situ RNA profiling by sequential hybridization. *Nat. Methods* 11:360–61
82. Marguerat S, Schmidt A, Codlin S, Chen W, Aebersold R, Bahler J. 2012. Quantitative analysis of fission yeast transcriptomes and proteomes in proliferating and quiescent cells. *Cell* 151:671–83
83. Martin RM, Rino J, Carvalho C, Kirchhausen T, Carmo-Fonseca M. 2013. Live-cell visualization of pre-mRNA splicing with single-molecule sensitivity. *Cell Rep.* 4:1144–55
84. Mellis IA, Gupte R, Raj A, Rouhanifard SH. 2017. Visualizing adenosine-to-inosine RNA editing in single mammalian cells. *Nat. Methods* 14:801–4
85. Messier V, Zenklusen D, Michnick SW. 2013. A nutrient-responsive pathway that determines M phase timing through control of B-cyclin mRNA stability. *Cell* 153:1080–93
86. Moffitt JR, Hao J, Bambah-Mukku D, Lu T, Dulac C, Zhuang X. 2016. High-performance multiplexed fluorescence in situ hybridization in culture and tissue with matrix imprinting and clearing. *PNAS* 113:14456–61
87. Moor AE, Golan M, Massasa EE, Lemze D, Weizman T, et al. 2017. Global mRNA polarization regulates translation efficiency in the intestinal epithelium. *Science* 357:1299–303
88. Mor A, Suliman S, Ben-Yishay R, Yunger S, Brody Y, Shav-Tal Y. 2010. Dynamics of single mRNP nucleocytoplasmic transport and export through the nuclear pore in living cells. *Nat. Cell Biol.* 12:543–52
89. Morisaki T, Lyon K, DeLuca KF, DeLuca JG, English BP, et al. 2016. Real-time quantification of single RNA translation dynamics in living cells. *Science* 352:1425–29
90. Morisaki T, Müller WG, Golob N, Mazza D, McNally JG. 2014. Single-molecule analysis of transcription factor binding at transcription sites in live cells. *Nat. Commun.* 5:4456
91. Mueller F, Senecal A, Tantale K, Marie-Nelly H, Ly N, et al. 2013. FISH-quant: automatic counting of transcripts in 3D FISH images. *Nat. Methods* 10:277–78
92. Mueller F, Stasevich TJ, Mazza D, McNally JG. 2013. Quantifying transcription factor kinetics: at work or at play? *Crit. Rev. Biochem. Mol. Biol.* 48:492–514
93. Munsky B, Neuert G, van Oudenaarden A. 2012. Using gene expression noise to understand gene regulation. *Science* 336:183–87
94. Muzzey D, Sherlock G, Weissman JS. 2014. Extensive and coordinated control of allele-specific expression by both transcription and translation in *Candida albicans*. *Genome Res.* 24:963–73
95. Nelles DA, Fang MY, O'Connell MR, Xu JL, Markmiller SJ, et al. 2016. Programmable RNA tracking in live cells with CRISPR/Cas9. *Cell* 165:488–96
96. Paige JS, Wu KY, Jaffrey SR. 2011. RNA mimics of green fluorescent protein. *Science* 333:642–46
97. Park HY, Buxbaum AR, Singer RH. 2010. Single mRNA tracking in live cells. *Methods Enzymol.* 472:387–406

98. Park HY, Lim H, Yoon YJ, Follenzi A, Nwokafor C, et al. 2014. Visualization of dynamics of single endogenous mRNA labeled in live mouse. *Science* 343:422–24
99. Parker R. 2012. RNA degradation in *Saccharomyces cerevisae*. *Genetics* 191:671–702
100. Paulsson J. 2004. Summing up the noise in gene networks. *Nature* 427:415–18
101. Pelechano V, Wei W, Steinmetz LM. 2015. Widespread co-translational RNA decay reveals ribosome dynamics. *Cell* 161:1400–12
102. Pérez-Ortín JE, Alepuz P, Chávez S, Choder M. 2013. Eukaryotic mRNA decay: methodologies, pathways, and links to other stages of gene expression. *J. Mol. Biol.* 425:3750–75
103. Pichon X, Bastide A, Safieddine A, Chouaib R, Samacoits A, et al. 2016. Visualization of single endogenous polysomes reveals the dynamics of translation in live human cells. *J. Cell Biol.* 214:769–81
104. Raj A, Peskin CS, Tranchina D, Vargas DY, Tyagi S. 2006. Stochastic mRNA synthesis in mammalian cells. *PLOS Biol.* 4:e309
105. Raj A, van den Bogaard P, Rifkin SA, van Oudenaarden A, Tyagi S. 2008. Imaging individual mRNA molecules using multiple singly labeled probes. *Nat. Methods* 5:877–79
106. Raj A, van Oudenaarden A. 2008. Nature, nurture, or chance: stochastic gene expression and its consequences. *Cell* 135:216–26
107. Raser JM, O'Shea EK. 2004. Control of stochasticity in eukaryotic gene expression. *Science* 304:1811–14
108. Rodriguez EA, Campbell RE, Lin JY, Lin MZ, Miyawaki A, et al. 2017. The growing and glowing toolbox of fluorescent and photoactive proteins. *Trends Biochem. Sci.* 42:111–29
109. Sanchez A, Golding I. 2013. Genetic determinants and cellular constraints in noisy gene expression. *Science* 342:1188–93
110. Saroufim MA, Bensidoun P, Raymond P, Rahman S, Krause MR, et al. 2015. The nuclear basket mediates perinuclear mRNA scanning in budding yeast. *J. Cell Biol.* 211:1131–40
111. Schmidt U, Basyuk E, Robert MC, Yoshida M, Villemin JP, et al. 2011. Real-time imaging of cotranscriptional splicing reveals a kinetic model that reduces noise: implications for alternative splicing regulation. *J. Cell Biol.* 193:819–29
112. Schwanhausser B, Busse D, Li N, Dittmar G, Schuchhardt J, et al. 2011. Global quantification of mammalian gene expression control. *Nature* 473:337–42
113. Senecal A, Munsky B, Proux F, Ly N, Braye FE, et al. 2014. Transcription factors modulate c-Fos transcriptional bursts. *Cell Rep.* 8:75–83
114. Sepulveda LA, Xu H, Zhang J, Wang M, Golding I. 2016. Measurement of gene regulation in individual cells reveals rapid switching between promoter states. *Science* 351:1218–22
115. Shaffer SM, Wu M-T, Levesque MJ, Raj A. 2013. Turbo FISH: a method for rapid single molecule RNA FISH. *PLOS ONE* 8:e75120
116. Shah P, Ding Y, Niemczyk M, Kudla G, Plotkin JB. 2013. Rate-limiting steps in yeast protein translation. *Cell* 153:1589–601
117. Shaw LB, Sethna JP, Lee KH. 2004. Mean-field approaches to the totally asymmetric exclusion process with quenched disorder and large particles. *Phys. Rev. E* 70:021901
118. Shorter J. 2016. Membraneless organelles: phasing in and out. *Nat. Chem.* 8:528–30
119. Siebrasse JP, Kaminski T, Kubitscheck U. 2012. Nuclear export of single native mRNA molecules observed by light sheet fluorescence microscopy. *PNAS* 109:9426–31
120. Singh G, Pratt G, Yeo GW, Moore MJ. 2015. The clothes make the mRNA: past and present trends in mRNP fashion. *Annu. Rev. Biochem.* 84:325–54
121. Skinner SO, Sepulveda LA, Xu H, Golding I. 2013. Measuring mRNA copy number in individual *Escherichia coli* cells using single-molecule fluorescent in situ hybridization. *Nat. Protoc.* 8:1100–13
122. Smith CS, Lari A, Derrer CP, Ouwehand A, Rossouw A, et al. 2015. In vivo single-particle imaging of nuclear mRNA export in budding yeast demonstrates an essential role for Mex67p. *J. Cell Biol.* 211:1121–30
123. Smith CS, Preibisch S, Joseph A, Abrahamsson S, Rieger B, et al. 2015. Nuclear accessibility of β-actin mRNA is measured by 3D single-molecule real-time tracking. *J. Cell Biol.* 209:609–19
124. Speese SD, Ashley J, Jokhi V, Nunnari J, Barria R, et al. 2012. Nuclear envelope budding enables large ribonucleoprotein particle export during synaptic Wnt signaling. *Cell* 149:832–46

125. Stasevich TJ, Hayashi-Takanaka Y, Sato Y, Maehara K, Ohkawa Y, et al. 2014. Regulation of RNA polymerase II activation by histone acetylation in single living cells. *Nature* 516:272–75
126. Strack RL, Disney MD, Jaffrey SR. 2013. A superfolding Spinach2 reveals the dynamic nature of trinucleotide repeat-containing RNA. *Nat. Methods* 10:1219–24
127. Subramaniam AR, Zid BM, O'Shea EK. 2014. An integrated approach reveals regulatory controls on bacterial translation elongation. *Cell* 159:1200–11
128. Suter DM, Molina N, Gatfield D, Schneider K, Schibler U, Naef F. 2011. Mammalian genes are transcribed with widely different bursting kinetics. *Science* 332:472–74
129. Takahashi K, Yamanaka S. 2006. Induction of pluripotent stem cells from mouse embryonic and adult fibroblast cultures by defined factors. *Cell* 126:663–76
130. Takizawa PA, Vale RD. 2000. The myosin motor, Myo4p, binds Ash1 mRNA via the adapter protein, She3p. *PNAS* 97:5273–78
131. Tanenbaum ME, Gilbert LA, Qi LS, Weissman JS, Vale RD. 2014. A protein-tagging system for signal amplification in gene expression and fluorescence imaging. *Cell* 159:635–46
132. Taniguchi Y, Choi PJ, Li G-W, Chen H, Babu M, et al. 2010. Quantifying *E. coli* proteome and transcriptome with single-molecule sensitivity in single cells. *Science* 329:533–38
133. Tantale K, Mueller F, Kozulic-Pirher A, Lesne A, Victor JM, et al. 2016. A single-molecule view of transcription reveals convoys of RNA polymerases and multi-scale bursting. *Nat. Commun.* 7:12248
134. Trcek T, Larson DR, Moldon A, Query CC, Singer RH. 2011. Single-molecule mRNA decay measurements reveal promoter-regulated mRNA stability in yeast. *Cell* 147:1484–97
135. Trcek T, Sato H, Singer RH, Maquat LE. 2013. Temporal and spatial characterization of nonsense-mediated mRNA decay. *Genes Dev.* 27:541–51
136. Tsai A, Muthusamy AK, Alves MR, Lavis LD, Singer RH, et al. 2017. Nuclear microenvironments modulate transcription from low-affinity enhancers. *eLife* 6:e28975
137. Tutucci E, Stutz F. 2011. Keeping mRNPs in check during assembly and nuclear export. *Nat. Rev. Mol. Cell Biol.* 12:377–84
138. Tutucci E, Vera M, Biswas J, Garcia J, Parker R, Singer RH. 2018. An improved MS2 system for accurate reporting of the mRNA life cycle. *Nat. Methods* 15:81–89
139. Tyagi S, Kramer FR. 1996. Molecular beacons: probes that fluoresce upon hybridization. *Nat. Biotechnol.* 14:303–8
140. Wang C, Han B, Zhou R, Zhuang X. 2016. Real-time imaging of translation on single mRNA transcripts in live cells. *Cell* 165:990–1001
141. Wu B, Buxbaum AR, Katz ZB, Yoon YJ, Singer RH. 2015. Quantifying protein-mRNA interactions in single live cells. *Cell* 162:211–20
142. Wu B, Chao JA, Singer RH. 2012. Fluorescence fluctuation spectroscopy enables quantitative imaging of single mRNAs in living cells. *Biophys. J.* 102:2936–44
143. Wu B, Eliscovich C, Yoon YJ, Singer RH. 2016. Translation dynamics of single mRNAs in live cells and neurons. *Science* 352:1430–35
144. Xu H, Sepulveda LA, Figard L, Sokac AM, Golding I. 2015. Combining protein and mRNA quantification to decipher transcriptional regulation. *Nat. Methods* 12:739–42
145. Xu H, Skinner SO, Sokac AM, Golding I. 2016. Stochastic kinetics of nascent RNA. *Phys. Rev. Lett.* 117:128101
146. Yan X, Hoek TA, Vale RD, Tanenbaum ME. 2016. Dynamics of translation of single mRNA molecules in vivo. *Cell* 165:976–89
147. Yang L, Titlow J, Ennis D, Smith C, Mitchell J, et al. 2017. Single molecule fluorescence in situ hybridisation for quantitating post-transcriptional regulation in *Drosophila* brains. *Methods* 126:166–76
148. Yoon YJ, Wu B, Buxbaum AR, Das S, Tsai A, et al. 2016. Glutamate-induced RNA localization and translation in neurons. *PNAS* 113:E6877–86
149. Yuan GC, Cai L, Elowitz M, Enver T, Fan G, et al. 2017. Challenges and emerging directions in single-cell analysis. *Genome Biol.* 18:84
150. Zenklusen D, Larson DR, Singer RH. 2008. Single-RNA counting reveals alternative modes of gene expression in yeast. *Nat. Struct. Mol. Biol.* 15:1263–71

151. Zhang J, Fei J, Leslie BJ, Han KY, Kuhlman TE, Ha T. 2015. Tandem Spinach array for mRNA imaging in living bacterial cells. *Sci. Rep.* 5:17295
152. Zhao R, Nakamura T, Fu Y, Lazar Z, Spector DL. 2011. Gene bookmarking accelerates the kinetics of post-mitotic transcriptional re-activation. *Nat. Cell Biol.* 13:1295–304
153. Zia RKP, Dong JJ, Schmittmann B. 2011. Modeling translation in protein synthesis with TASEP: a tutorial and recent developments. *J. Stat. Phys.* 144:405–28

Annual Review of Biophysics
Volume 47, 2018

Contents

Indexes

Errata

An online log of corrections to *Annual Review of Biophysics* articles may be found at http://www.annualreviews.org/errata/biophys